Volume 2 • Number 4 • June 2008
ISSN: 1557-7244

Journal of

APPLIED PACKAGING RESEARCH

Aim and Scope

The *Journal of Applied Packaging Research* is an international forum for the dissemination of research papers, review articles, tutorials and news about innovative or emerging technologies for the packaging industry. The journal is targeted towards the broad packaging community including packaging scientists and engineers in industry or academic research and development, food scientists and technologists, materials scientists, mechanical engineers, industrial and systems engineers, toxicologists, analytical chemists, environmental scientists, regulatory officers, and other professionals who are concerned with advances in the development and applications of packaging.

JOURNAL OF APPLIED PACKAGING RESEARCH—Published quarterly—September, December, March and June by DEStech Publications, Inc., 439 North Duke Street, Lancaster, PA 17602-4967.

This journal is recommended by The National Institute of Packaging Handling and Logistics Engineers (www.niphle.org).

Indexed by Chemical Abstracts Service.

Indexed and abstracted by Pira International.

Subscriptions: Annual $299 (Print), $299 (Electronic) and $324 (Print and Electronic). Single copy price $89.50. Foreign subscriptions add $45 per year for postage.

(ISSN 1557-7244)

DES*tech* Publications, Inc.
439 North Duke Street, Lancaster, PA 17602-4967, U.S.A.

CONTENTS

Determining the Minimum Sample Size Using a Simplified Method for Determining Cushion Curves

PATRICIA D.G. MARCONDES*, GREGORY S. BATT,
DUNCAN DARBY and MATT DAUM
Clemson University, Department of Packaging Science, Clemson, South Carolina

ABSTRACT: Traditional methods of producing cushion curves require significant resources in time and materials. A new method of developing cushion curves based on the stress-energy method has proven to greatly reduce the number of required samples when compared to traditional methods (Burgess, 1990). This paper addresses the question of what is the minimum number of samples that are statistically necessary to characterize the shock absorbing properties of closed-cell foams. Cushion materials were evaluated using the stress-energy method, the data was statistically analyzed, and an optimum number of samples was determined.

1.0 INTRODUCTION

THE work done by Dr. Gary Burgess on the consolidation of cushion curves of closed-cell foams was published in 1990 (Burgess, 1990). It explains how to summarize the cushioning properties of a given material into one curve which offers a continuous range of application. One of the conclusions from the work is that far fewer drops are needed to construct the stress-energy curve for a given material than are needed to construct a full set of traditional cushion curves.

A simplified process for determining cushion curves for closed cell foams was presented at Dimensions '06 (Daum, 2006). Dr. Daum showed that curves based on the stress-energy relationship could be produced with a quarter of the data necessary to produce traditional cushion curves. Benefits in terms of savings in laboratory time, sample preparation, and the continuous range nature of the curve could be realized by using this method for evaluating the cushioning properties of the closed-cell foams.

*Author to whom correspondence should be addressed.

1557-7244/07/04 191-07

The analysis presented in this paper investigates the question of the minimum sample size needed to adequately characterize a given material using the stress-energy equation.

BACKGROUND

The test procedure used for collecting the deceleration data for the stress-energy method followed the guidelines of ASTM D-1596 "Test Method for Dynamic Shock Cushioning Characteristics of Packaging Material", which is also used as the current standard method for comparing the properties of closed-cell materials. However, only hundreds of drops per material density were needed versus the thousands needed when traditional cushion curve sets are drawn using ASTM D-1596. Using the stress-energy method, the shock absorbing property of a closed-cell material can be defined by the following equation:

$$y = ae^{bx} \tag{1}$$

Variables x and y are derived from testing, where y corresponds to dynamic stress and is defined by:

$$y = G \times s$$

where G is peak deceleration in units of g, and s is static loading (lb/in^2) and x corresponds to dynamic energy and is defined by:

$$x = \frac{s \times h}{t}$$

where s is static loading (lb/in^2), h is equivalent drop height (in), and t is sample thickness (in)

Parameters a and b are calculated by fitting a line to the data points. According to Daum's analysis, the lines for the four different material densities tested all had a correlation coefficient (R^2) above 0.90. The equations resulting from the line fitting were used to draw cushion curves for any thickness, static load, and drop height (Daum, 2006). With traditional cushion curves, one is limited to deceleration response values at discrete drop heights and thicknesses. The stress-energy method allows the creation of a formula (Equation 1) specific to a given material that allows the deceleration response to be determined at any selected drop height, thickness, and static loading.

EXPERIMENTS PERFORMED

The testing procedure utilized combinations of drop height, sample thickness and static loading which produced 10 to12 energy values ranging from a minimum of 5 in-lb/in^3 to maximums of 50 or 80 in-lb/in^3 (depending on foam density). Five replicates per energy level were tested. Each replicate received five impacts. The materials used were provided by NOVA Chemicals Inc. and consisted of four different densities: 1.2, 1.7, 2.2, and 3.0 lb/ft^3. Molded and fabricated samples of 1.2 and 2.2 lb/ft^3 were tested for a total of six data sets. Table 1 shows a summary of drops performed. Four material densities were fully characterized, with respect to their deceleration response. This was done with fewer drops than would be necessary to produce a single set of cushion curves for one material density, if using ASTM D-1596. Fewer than the planned drops were ultimately analysed because of anomalies in the data collection process, such as failure to capture the shock pulse due to equipment sensitivities and trigger thresholds.

Figure 1 illustrates the scatter plot of the data collected for a particular density. In keeping with current cushion curve convention, equations were generated for the first impact data and for the average of 2nd to 5th drops. In order to protect the proprietary information of NOVA Chemicals Inc., the equation coefficients and the material identity have been omitted from this work.

It is visually apparent from the scatter plot that the XY relationship is exponentially increasing. It is also visually apparent that the spread within each of the higher energy values was much greater than at the lower values. The data was transformed with the objective of linearizing the relationship to make common statistical analyses possible. Ott and Longnecker (2001) recommend transforming the dependent variable us-

Table 1. *Summary of Drops Performed.*

Tag	Energy Values	Number of drops Planned	Number of drops Analysed
1.2 (lb/ft^3) Molded	10	250	220
1.2 (lb/ft^3) Fabricated	10	250	230
1.7 (lb/ft^3) Molded	10	250	240
2.2 (lb/ft^3) Molded	12	300	275
2.2 (lb/ft^3) Fabricated	12	300	265
3.0 (lb/ft^3) Molded	12	300	265

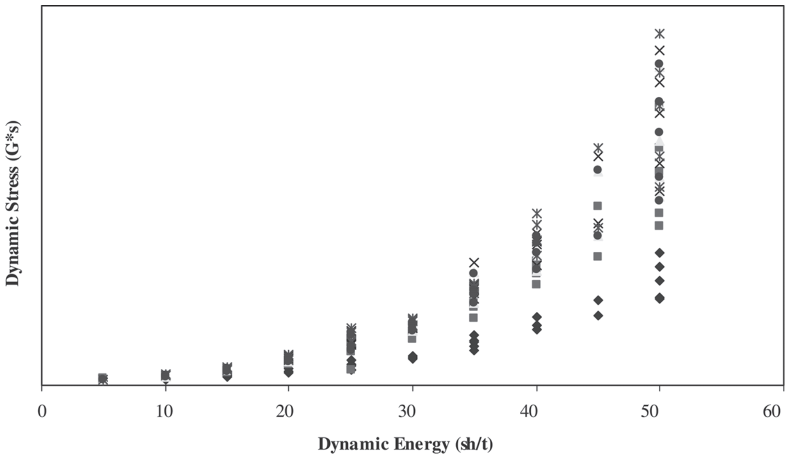

Figure 1. *Scatter plot of all data for one material density.*

ing the natural logarithm, ln(y), to linearize an exponentially increasing relationship. Figure 2 shows the data in Figure 1 after the natural log transformation linearization.

The transformation showed data points that were spread linearly, and with normally distributed variances for five of the six data sets. The data set for the 3.0 lb/ft^3 data did not look as linear as the others, with a correlation coefficient of 0.86 for the first impact data. Therefore, it was eliminated from further analysis.

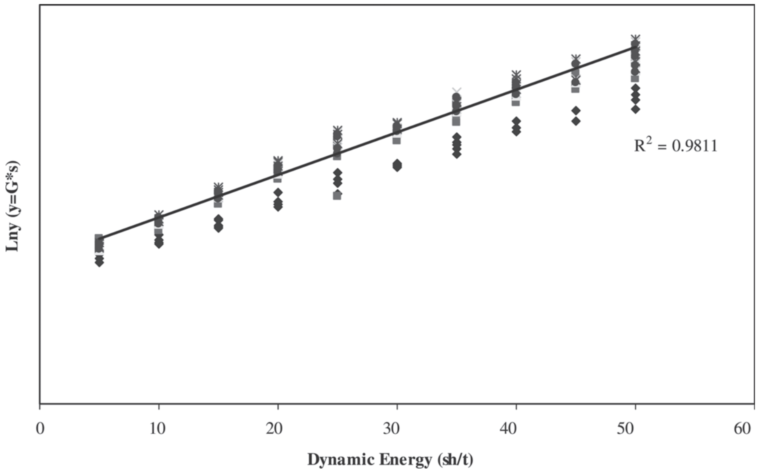

Figure 2. *Scatter plot of transformed data.*

The data for each remaining material was divided into first impact data and average of 2nd to 5th impact data, according to current industry convention. A statistical software package, SAS 9.1, was used to fit a line where x (dynamic energy) was the independent variable, and $\ln(y)$ was the dependent variable. From this modeling, least-squares estimates of the slope and intercept of the fitted lines were obtained.

Since basic geometry dictates that only two points are necessary to define a line, the theory that one might be able to describe the relationship between x and $\ln(y)$ using the results obtained for two values of x was tested by fitting lines through all the data points available, and fitting lines to data points corresponding to two values of $\ln(y)$. This would reduce the number of samples needed per material density to 10 and the number of drops to 50 when 5 impacts per sample were performed.

Two extremes of x (dynamic energy) were chosen for each of the five densities tested. The line parameters a and b, from the line fitted using these extremes were compared to those parameters from the line fitted using the entire range of x values. The comparison made was a t-test with $\alpha = 0.05$. Lines were fitted for both the first impact data and averaged 2nd to 5th impact data.

RESULTS AND CONCLUSIONS

The transformed data for the 5 data sets under analysis indicated that the higher energy values were affecting the line parameters (intercept and slope). These same energy values also occur at combinations of static loading, drop height, and thickness which would be outside of practical values. The transmitted deceleration recorded was above the maximum values that can be found in product fragility tables (Soroka,1999). Therefore, these higher energy values were eliminated before the lines were fitted to the linearized data.

Figure 3 shows the plots of two pairs of lines obtained by regression analysis. Lines 1 and 3 were determined using the range of energy values available, and Lines 2 and 4 were determined using two values of energy.

A statistical comparison of the intercepts and slopes was performed to compare the slopes of the lines in Figure 3, as well as for the other four sets of data. The slope and the intercept of Lines 1 and 3 were compared to the slope and intercept of Lines 2 and 4, respectively for each of the material density tested. The t-test was used, with $\alpha = 0.05$. No statistical

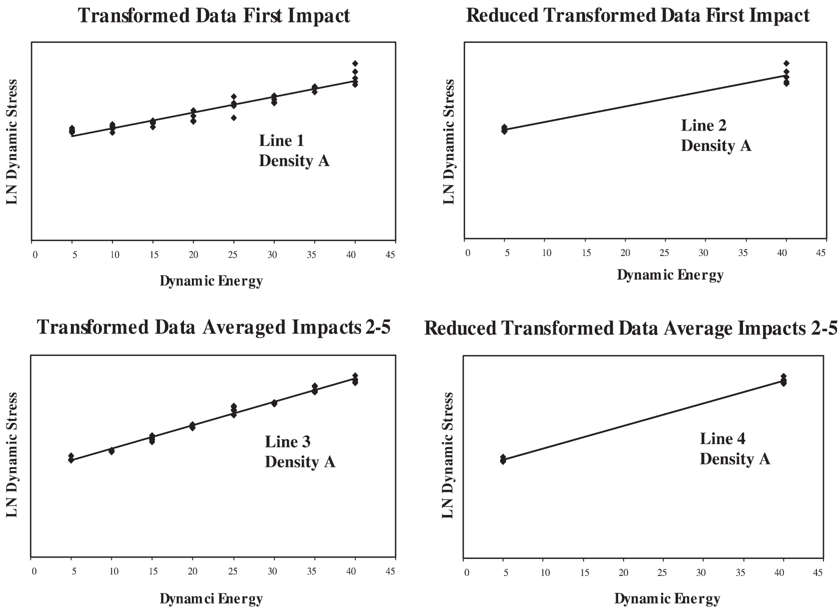

Figure 3. *Lines produced with range of energy values versus two energy values.*

difference in the parameters for the lines of two of the densities tested was found. But the other three pairs of lines showed statistical difference for at least one of the parameters (intercept or slope).

One more energy value was added to the middle of the range for a total of three energy levels per data set. Lines were fitted and the statistical comparisons were performed. Table 2 summarizes the results of the statistical analysis of the parameters for the lines fitted using three energy levels.

Table 2. *Summary of Statistical Comparison.*

	Results of Statistical Comparison (α = 0.05)			
	1st Impact		Averaged 2nd–5th Impacts	
Densities	**Intercept**	**Slope**	**Intercept**	**Slope**
1.2 (lb/ft^3) Molded	No Stat. Diff.	No Stat. Diff.	No Stat. Diff.	No Stat. Diff.
1.2 (lb/ft^3) Fabricated	No Stat. Diff.	No Stat. Diff.	No Stat. Diff.	No Stat. Diff.
1.7 (lb/ft^3) Molded	No Stat. Diff.	No Stat. Diff.	No Stat. Diff.	No Stat. Diff.
2.2 (lb/ft^3) Molded	No Stat. Diff.	No Stat. Diff.	No Stat. Diff.	No Stat. Diff.
2.2 (lb/ft^3) Fabricated	No Stat. Diff.	No Stat. Diff.	No Stat. Diff.	No Stat. Diff.

These results indicate that with 15 samples and 5 drops per sample per material a line can be fitted that can predict the transmitted deceleration of any typical combination of drop height, thickness and static loading for a closed-cell cushioning material.

In this work, the choice of energy levels was done simply by picking the two extreme values from the transformed data plus the mid-point. Further investigation is needed on how a choice should be made when no information about a material is available. When starting with a new material, it may be necessary to use predictors, such as compressibility or stress-strain behavior, to select the three energy levels for testing.

FUTURE WORK AND RECOMMENDATIONS

There are obvious time and expense benefits to the stress-energy method, but the limits of its application must be fully evaluated to make this a useful tool in augmenting the current ASTM D-1596 in evaluating the Dynamic Shock Cushioning Characteristics of Packaging Material.

More work needs to be done to evaluate the effectiveness of the dynamic stress-energy model in evaluating the cushioning properties of high density materials and extreme thicknesses and static loading.

Work is already under way at Clemson University to test the three-energy-level approach with other materials for comparison to existing cushion curves. Another approach to reducing data points, which includes fewer replicates within a range of energy values is also being evaluated.

REFERENCES

Burgess, G. "Consolidation of Cushion Curves." *Packaging Technology and Science* Vol, 3, 189–194 (1990).

Daum, M. (2006). A simplified process for determining cushion curves: The stress-energy method. *Proceedings from Dimensions '06*, San Antonio, TX.

Ott, R. L. and Longnecker, M (2001). *An Introduction to Statistical Methods and Data Analysis,* 5th ed. Wadsworth Group.

Soroka, W. (1999). *Fundamentals of Packaging Technology* (2nd ed.). Herndon, VA:IoPP.

Biodegradation of Steam-Treated Polylactic Acid (PLA) Under Composting Conditions

L. F. VARGAS, B. A. WELT* and P. PULLAMMANAPPALLIL

Agricultural & Biological Engineering Department, University of Florida/IFAS, Gainesville FL.

ABSTRACT: Biodegradation of steam-treated thermoformed polymer polylactic acid (PLA) under composting conditions was investigated. Treatments involved subjecting plastic PLA samples to steam at 120°C for 0, 1, 2, 3 and 4 hours. Ground steam-treated PLA was mixed with compost, filled in perforated jars, and assessed for biodegradation at 58°C via the "Method of Perforated Jars" developed in this work. Kinetics of PLA biodegradation in compost were adjusted to the logistic model with three parameters. To assess effectiveness of steam treatment, weight loss of PLA samples was determined in compost for 14 days. Degradation rates were compared with those of corrugated paperboard and virgin wood. Results showed that steam treatment is an excellent method to increase PLA biodegradation rate in subsequent composting processes. Increased performance was attributed to both "head start" and "acceleration" effects. Ground and treated PLA (120°C × 3h) achieved 60% of biodegradation after 14 days in compost. Flat sheets of treated PLA (120°C × 4h) degraded faster than wood and corrugated paperboard, loosing up to 94.9% of initial weight after 14 days in compost. The logistic model fit experimental data of PLA biodegradation well. Significant findings of this work are the shortening of compostability time of steam-treated PLA, and the development of a convenient method to assess biodegradation of polymers under composting conditions, which is referred to as the "method of perforated jars."

INTRODUCTION

POLYLACTIC ACID (PLA) is a biobased polymer derived from renewable resources, such as corn, and able to biodegrade to carbon dioxide and water (Drumright, 2000). Compostability of PLA has been discussed by different authors, and the agreement is that it occurs at temperatures around 58°C after several weeks (Kale et al., 2006;

*Author to whom correspondence should be addressed. Email: bwelt@ufl.edu

1557-7244/07/04 199-14

Massardier-Nageotte et al., 2006; Greer, 2006). Nevertheless, time to complete PLA breakdown may be too long compared with time frame of typical organic feedstock, and represents a potential bottleneck to composting operations. Commercial PLA packages have been shown to be incompletely degraded after 28 days of composting (Kale et al., 2006; Massardier-Nageotte et al., 2006).

Reactions that occur during PLA biodegradation in a composting process occur in three stages summarized in Figure 1. First, PLA hydrolyzes producing lower molecular weight PLA. This stage requires water and energy, but the presence of microorganisms is not essential. Then, low molecular weight PLA hydrolyzes further to produce oligomers and lactic acid. During this second stage, biological activity joins hydrolysis in breaking down PLA and is aided by appropriate temperature, moisture and oxygen levels. The third stage is carried out only by biological activity and produces carbon dioxide and water (Lunt, 1998). Depending on pH and specific microbes present, radicals may also be produced and combined with the biomass to integrate humic acids in the compost. Also, a small part of the carbon dioxide fraction dissolves in wet compost forming carbonic acid and carbonates.

The motivating hypothesis of this work is that treatments capable of disrupting the polymer matrix and/or reducing molecular weight should result in reduced overall composting time. Additionally, in the event that composting time is reduced, experiments were designed to determine whether pretreatments accelerated conversion kinetics or simply provided a head start to the composting process that subsequently proceeded at the typical rate. Means by which biodegradation time is shortened are graphically described in Figure 2. The “head start” effect is shown in Figure 2. A typical curve representing PLA biodegradation in the composting process can be described through 3 phases: (a) a lag period, (b) an accelerated biodegradation phase, and (c) a decelerated biodegradation phase until reaching a plateau. A “head start” effect

$$\text{PLA} \xrightarrow{\text{Heat, } O_2\text{, moisture}} \text{PLA (low } M_w\text{)}$$

$$\text{PLA (low } M_w\text{)} \xrightarrow{\text{Heat, mo, } O_2\text{, moisture}} \text{Oligomers + lactic acid}$$

$$\text{Oligomers, lactic acid} \xrightarrow{\text{Heat, mo, } O_2\text{, moisture}} CO_2 + H_20$$

Figure 1. *Main reactions in PLA biodegradation.*

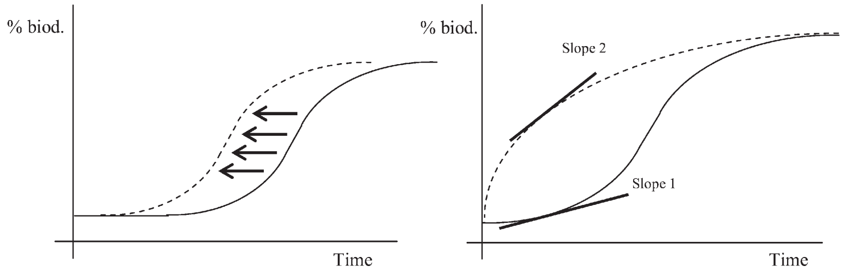

Figure 2. *Means to reduce biodegradation time. Left: head start effect; right: acceleration effect.*

would shift the curve in time, so that the lag period would be shortened or eliminated, but the trend of the curve would be maintained. So, a "head start" effect would be expected to displace the entire curve to the left. As a consequence of this "head start" effect, overall biodegradation time will be reduced. The "acceleration" effect is also illustrated in Figure 2. Here, biodegradation rate must be carefully analyzed once the lag period is complete. The slope of the curve (in the earlier phase) represents initial biodegradation rate, and is an indicator of how rapidly carbon dioxide is evolving. The dashed curve depicts biodegradation evolution of PLA exhibiting the "acceleration" effect, represented by a steeper slope.

The main objective of this research was to evaluate effects of steam treatments on kinetics of subsequent PLA aerobic biodegradation, and to determine whether or not treatment will allow PLA to completely degrade within the time frame of normal organic feedstock. Determination of PLA biodegradation in compost was performed via the "method of perforated jars" described in this work.

MATERIALS AND METHODS

Material

Thermoformed PLA drinking cups (Fabri-Kal, Inc., Kalamazoo, MI) were obtained from TREEO Center at the University of Florida. Cup dimensions were measured using a caliper (Mitutoyo Model CD-6 CS, Mitutoyo Corp., Japan) and are provided in Figure 3. Wall thicknesses were 150–200 µm and bottoms were about 750µm.

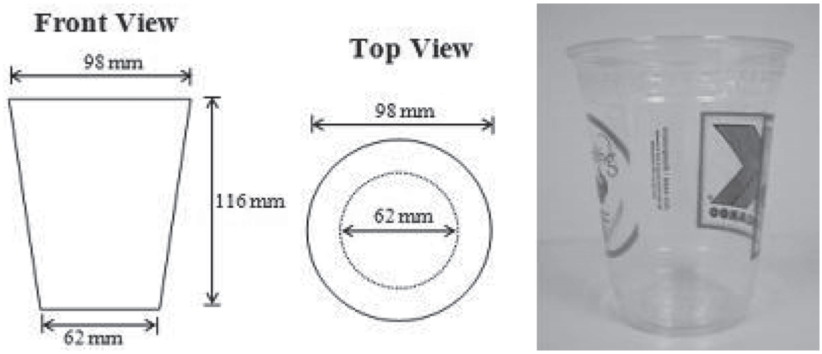

Figure 3. *Drinking cup made of PLA.*

STEAM TREATMENT OF PLA

Drinking cups of PLA were prepared as flat sheets and ground using an Urschel 3600 grinder (Urschel Laboratories, Inc., Valparaiso, IN) with a 3 mm screen. Ground PLA and flat sheets were placed inside jars. Lids of jars were adapted with two holes (about 1 cm diameter) to allow steam transfer. Jars were placed in a vertical still retort where steam was fed and temperature controlled with a pneumatic system. Samples of ground PLA remained in the retort for 1, 2 and 3 hours at 120°C. Flat sheets of PLA remained for 3 and 4 hours at 120°C. After treatment, samples were quickly cooled in air to room temperature and dried in an oven at 105°C until constant weight. Molecular weight of steam-treated PLA was determined using the method of intrinsic viscosity in accordance to ASTM D2857 (ASTM, 1996), using chloroform at 30°C as solvent and a calibrated capillary viscosimeter (Cannon-Ubbelodhe Type N°25, State College, PA). Constants for the Mark-Houwink model (Equation 1), which relates molecular weight, M, to the intrinsic viscosity, $[\mu]$, were $k = 0.0153$ml/g and $a = 0.759$ (Dorgan et al., 2005).

$$[\mu] = kM^{a} \tag{1}$$

Method of Perforated Jars

In perforated jars containing biomass (PLA-compost), oxygen enters through the holes to be consumed as part of the aerobic process. Biomass generates and releases carbon dioxide and water, which are diffused through the holes to the environment. A molar balance of carbon dioxide in the system can be written as in Equation 2.

$$\eta CO_2 \text{ generated} = \eta CO_2 \text{ diffused} + \eta CO_2 \text{ headspace} \quad (2)$$

The number of moles, η, diffused represents the average of moles flowing through the holes. This value can be estimated by Equation 3, derived from Fick's first law that states that the flux or rate of transport of an ideal gas is linearly related to its concentration gradient (Robertson, 2006).

$$\eta CO_2 \text{ diffused} = D_{ef}\,[CO_2]\,\Delta t \quad (3)$$

where D_{ef} is the overall effective coefficient of diffusion, $[CO_2]$ is the concentration of carbon dioxide, and Δt is the time interval between readings, which was 24 hours. Values of $[CO_2]$ were data recorded daily. Value of Def was determined experimentally and found to be 0.00031 moles/h/%. For this purpose, jars with similar features as those used for PLA biodegradation assessment were filled with 20 ml of DI water and some carbon dioxide. Jars were closed using the 5-hole perforated lids and stored at 58°C. Each 0.5 h, carbon dioxide concentration was determined in headspace and effusion rate values expressed as moles CO^2 effused per hour were estimated. The value of Def was obtained from the slope of the plot of effusion rate against $\%CO_2$ in headspace.

The number of moles in the headspace can be estimated by Equation 4 which is derived from the universal gas law (Tsimpanogiannis and Yortsos, 2002).

$$\eta CO_2 \text{ headspace} = \frac{p_{CO_2} V_{hs}}{RT} = \frac{p_{atm}[CO_2]V_{hs}}{RT} \quad (4)$$

where p_{CO_2} is the partial pressure of CO_2 in headspace, p_{atm} is the atmospheric pressure, V_{hs} is the free volume in headspace, R is the universal gas constant, and T is the absolute temperature. Volume of the headspace was estimated by subtracting the volume occupied by the biomass from the total volume of the jars.

Production of CO_2 solely from PLA is the difference between CO_2 produced from the mixture PLA-compost and CO_2 produced from the compost itself (control). The carbon mass can be determined by multiplying the number of moles of CO_2 produced by 12, which is the molecular weight of carbon. Finally, total biodegradation is the ratio of carbon mass evolved as CO_2 to initial carbon mass in PLA, and can be expressed as in Equation 5. From molecular weigh estimation, carbon mass in PLA is half of its total mass.

$$\%\text{biod.} = \frac{\text{Mass of carbon in evolved } CO_2}{\text{Mass of carbon in polymer}} \times 100\% \qquad (5)$$

STEAM-TREATED PLA BIODEGRADATION IN COMPOST

Ground steam-treated PLA at 120°C for 0, 1, 2 and 3 hours was used in this experiment. Mason jars of 936 cc capacity provided with 5 holes (× 1/16″) in the lids were filled with 100 g of 6-month mature compost and 10 g of ground PLA samples. Figure 4 shows pictures of the filled jar and perforated lid. Compost was originally developed using a standard organic matter feedstock recipe consisting of freshly cut grass (58%), saw

Figure 4. Jar filled with biomass and perforated lid.

dust (11%), virgin corrugated board (11%) and mature compost (20%). Controls were jars containing only 100 g of compost. Sealed jars were stored at 58°C for 31 days in a Lab-Line® L-C Incubator (Lab-Line Instruments, Inc., Melrose Park, IL). Beside routine practices such as agitation and moisturizing, concentration of gases in the headspace was determined daily using a gas analyzer Pac Check® 650 (Mocon, Inc., Minneapolis, MN). The "Method of Perforated Jars", based on principles of gas diffusion and developed in this work, was used to obtain kinetics of PLA biodegradation from data collected.

EMPRIRICAL MODEL FOR STEAM-TREATED PLA BIODEGRADATION IN COMPOST

Data of biodegradation were plotted and adjusted to the logistic model with three parameters shown in Equation 6. Parameters were estimated using nonlinear regression performed with SigmaPlot v.10. Ideally, parameter a should be 100. Parameter b is associated with the lag period, and the parameter x_o represents the time at which half of the biodegradation would be completed. For untreated PLA, large values of parameters b and x_o were expected, whereas for treated PLA smaller values were expected.

$$\%\text{biod.} = \frac{a}{1+(t/x_o)^{-b}} \tag{6}$$

WEIGHT LOSS OF STEAM-TREATED PLA IN COMPOST AND COMPARISON WITH OTHER COMMON FEEDSTOCK

Flat sheet samples of PLA treated with steam at 120°C for 3 and 4 hours were used for this experiment. They were cut in circular shapes (~12.5 cm^2) and wrapped in nylon screen envelopes. Also, flat sheets of same area made of wood and virgin corrugated paperboard were prepared. All samples from different materials were dried, weighed and immersed in water for 10 minutes. Wet samples were placed individually into perforated mason jars (capacity 936 cc) containing 200 g of 6-month mature compost. Closed jars were stored in a Lab-Line® L-C Incubator (Lab-Line Instruments, Inc., Melrose Park, IL) for 14 days at 58°C.

Periodically, jars were gently shaken to ensure uniform contact of samples with compost, and water was injected to maintain proper moisture content of the biomass. Samples were covered by the compost at all times to promote biological activity. At the end of the experiment, samples were removed from the jars, carefully washed, dried and weighted. Weight loss, w, of each individual sample was determined using Equation 7, where W is the final weight and W_o is the initial weight.

$$w = \frac{W_o - W}{W_o} \times 100\% \tag{7}$$

RESULTS AND DISCUSSIONS

Steam Treatment of PLA

Table 1 shows impacts of steam treatment on PLA molecular weight. As expected, longer treatment times resulted in lower molecular weights. Additionally, brittleness increased with increasing treatments.

Steam-Treated PLA Biodegradation in Compost

Figure 5 shows kinetics of steam-treated PLA biodegradation under composting conditions. On average, rates of biodegradation increased as steam treatment became more severe. These results confirm that a pre-composting treatment capable of reducing PLA molecular weight increases biodegradation rates in subsequent composting processes. This figure also suggests that both "head start" and "acceleration" effects contribute to overall enhanced biodegradation rates. As steam treatment increased, "head start" and "acceleration" effects also increased.

During experiments, oxygen concentration in the headspace was monitored and found to be at or above 18% at all times. Agitation permitted good aeration and mixing, and good agitation techniques were re-

Table 1. *Molecular Weight of Steam-treated PLA.*

Treatment	$M_w/M_{w,o}$ (%)
120°C x 1h	39.0
120°C x 2h	20.6
120°C x 3h	12.9
120°C x 4h	5.7

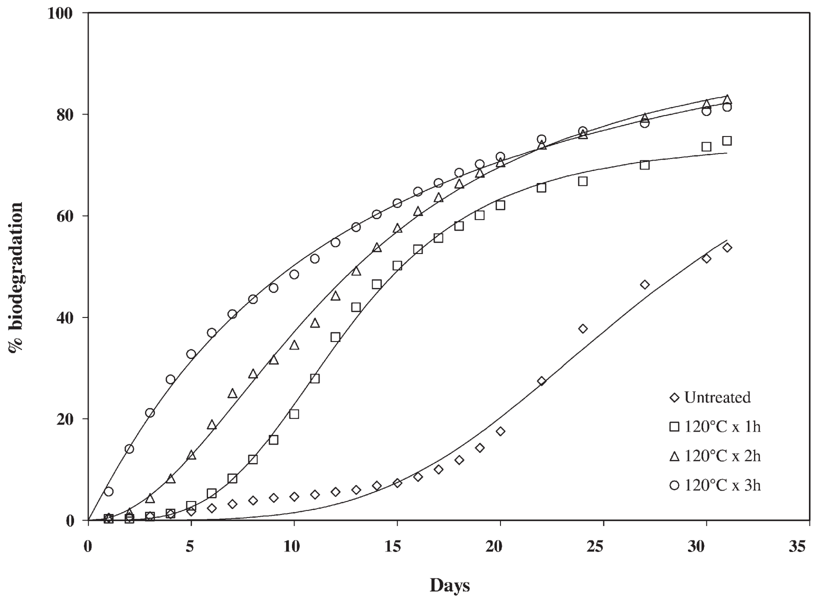

Figure 5. *Biodegradation of steam-treated PLA over time in compost.*

quired to minimize clumping. Unfortunately, clumping occurred in jars containing PLA treated with steam for 3 hours at 120°C during the last days of composting. Clumping appeared to slow biodegradation during those last days.

According to standards, "biodegradabililty" requires 60% conversion. In this regard, samples treated at 120°C for 3, 2 and 1 hours reached biodegradability after 14, 16 and 19 days, respectively. Untreated samples did not achieve biodegradability even after 31 days. Even when total biodegradation was not yet achieved, PLA had apparently disappeared, and it could be said that breakdown was complete. However, continued production of CO_2 attributed to PLA material suggests the presence of PLA, probably as oligomers, and lactic acid.

It was also observed that more severe treatments (i.e. 120°C × 3h) did not create a lag period for adaptation or conditioning. In these samples, the rate of biodegradation was very high at the beginning of the experiment and then decreased over time. In contrast, PLA samples less severely treated (i.e. 120°C × 1h) showed a sigmoidal behavior, represented by a lag period, accelerating and decelerating stage.

Materials must fulfill three conditions to be compostable (De Wilde

Table 2. *pH of Biomass (compost + biodegraded PLA).*

Sample	pH
Compost	6.7
Untreated	6.6
1h @ 120°C	6.6
2h @ 120°C	6.6
3h @ 120°C	6.8

and Boelens, 1998) including (1) rapid breakdown, (2) not modify compost usability, and (3) it must physically disintegrate. Samples of steam-treated PLA appear to have fulfilled these conditions. The 31-days biomass, consisting of biodegraded treated PLA in compost, had similar appearance, texture and odor as compost without PLA. The pH of the final biomass (~6.6–6.8) did not change (Table 2). Pictures of the compost with and without treated PLA are shown in Figure 6. There was no apparent difference between the two compost samples, although plant growth yield tests, which were not done in this study, may provide a definitive indication.

Empirical Model for Steam-Treated PLA Biodegradation in Compost

Nonlinear regression to fit experimental data to the logistic model was

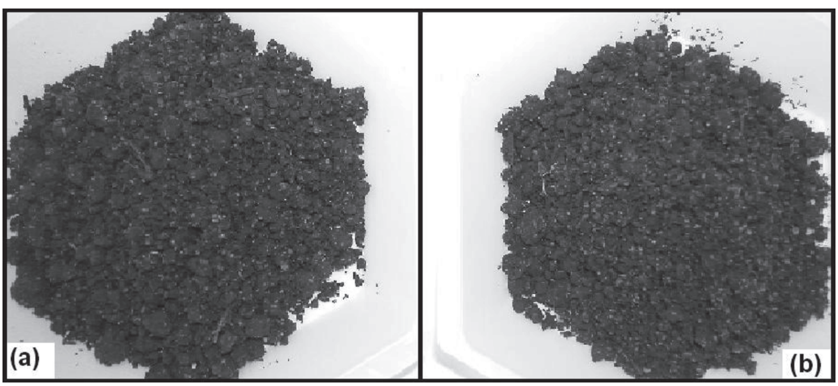

Figure 6. *Biodegraded PLA in compost: (a) compost by itself, (b) compost + PLA (not seen anymore).*

Table 3. *Parameters of the Logistic Model (%biod = a/(1 + (t/x_o)$^{-b}$).*

	Untreated	1h @ 120°C	2h @ 120°C	3h @ 120°C
a	84.01	75.15	96.91	113.80
b	4.103	3.612	2.04	1.05
xo	26.45	12.57	12.61	12.49
R-square	0.9819	0.9981	0.9981	0.9981

obtained using SigmaPlot v.10. Outputs are shown in Table 3. Parameters of the model are related with the pattern and magnitudes of the biodegradation curves.

Parameter *a* is the plateau, which is the maximum value of biodegradation that can be achieved. In all cases the value of a is close to 100, which is the theoretical plateau. The parameter *b* is associated with the lag period, so smaller values indicate shorter lag times. This matches experimental results, where more severe pretreatments resulted in lower values of *b* (for instance, steam-treated PLA at 120°C × 3h got the shortest value of *b*, and untreated PLA the highest). Finally, the parameter x_o is the time at which half of the biodegradation is completed. Thus, larger values of x_o indicate longer total times for biodegradation. Figure 5 shows that experimental data fit the model well.

Weight Loss of Steam-Treated PLA in Compost and Comparison with Other Common Feedstock

Figure 7 shows results of weight loss of steam-treated PLA, wood and virgin corrugated paperboard in 6-month mature compost. Treated PLA samples were the only ones that broke apart inside the compost. Screened envelopes were designed to retain broken parts for further weighting. After 14 days, steam-treated PLA achieved weight losses of 94.9% (120°C × 4h) and 86.4% (120°C × 3h), whereas wood and corrugated board achieved values of 0.9% and 39.2%, respectively. These results demonstrate that PLA subjected to steam (120°C × 3 and 4 h) breaks down much faster than wood and virgin corrugated paperboard, which are usually accepted in composting facilities. Figure 8 shows pictures of these samples, and it was observed that steam-treated PLA was most greatly affected.

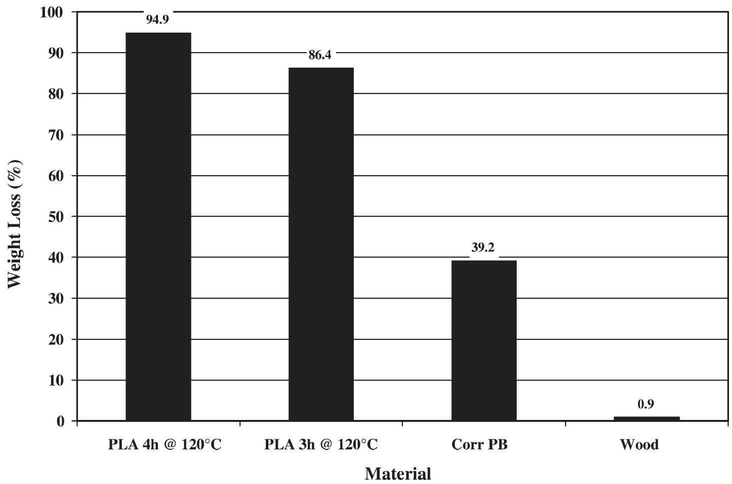

Figure 7. *Weight loss of steam-treated PLA in compost compared with corrugated board and wood.*

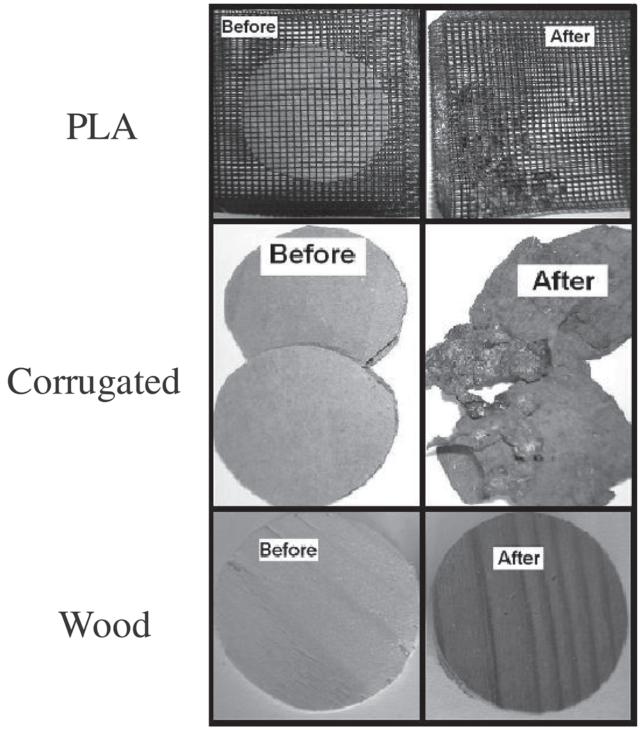

Figure 8. *Steam treated PLA (120°C x 3h), corrugated paperboard and wood subjected to compost for 14 days.*

CONCLUSION

It has been demonstrated that steam-treated PLA is affected significantly in compost, breaking down even faster than common organic feedstock universally accepted in composting facilities such as wood and virgin corrugated paperboard. Polylactic acid treated with steam at 120°C for 3, 2 and 1 hours, achieved degradability (60% of conversion to CO_2) after 14, 16 and 19 days, whereas untreated PLA did not achieve biodegradability even after 31 days.

Degradability was evidenced by complete PLA disappearance. Additionally, resulting compost did not appear to be affected by a loading of about 10% by weight PLA in compost.

Characteristics of the final compost when steam-treated PLA was initially present were similar than those of the compost by itself. PLA appeared to have met the three requirements for compostability including fast breakdown, total disintegration and no alteration.

Biodegradation kinetics of PLA fit very well using the proposed logistic model with three parameters, and provides valuable information for understanding biodegradation behavior. Determined parameters confirmed that pre-composting treatments that reduced PLA molecular weight provided "head start" and "acceleration" effects during subsequent composting process.

REFERENCES

American Society for Testing and Materials, 1996. ASTM D2857. Standard practice for dilute solution viscosity of polymers.

De Wilde B., J. Boelens. 1998. Prerequisites for biodegradable plastic materials for acceptance in real-life composting plants and technical aspects. *Polymer Degradation and Stability* 59(1–3): 7–12.

Dorgan J.R., J. Janzen, D. M. Knauss, S. B. Hait, B. Limoges, M. H. Hutchinson. 2005. Fundamental solution and single-chain properties of polylactides. *Journal of Polymer Science: Part B: Polymer Physics* 43: 3100–3111.

Drumright R.E., P. R. Gruber, D. E. Henton. 2000. Polylactic acid technology. *Advanced Materials* 12(23): 1841–1846.

Greer D. 2006. Plastics from plants, not petroleum. *Biocycle* 47(6): 33–35.

Kale G., R. Auras, S. Singh. Degradation of commercial biodegradable packages under real composting and ambient exposure conditions. *Journal of Polymers and the Environment* 14: 317–334.

Lunt J. 1998. Large-scale production, properties and commercial applications of polylactic acid polymers. Polymer Degradation and Stability 59(1-3): 145–152.

Massardier-Nageotte V., C. Pestre, T. Cruard-Pradet, R. Bayard. 2006. Aerobic and anaerobic biodegradability of polymer films and physico-chemical characterization. *Polymer Degradation and Stability* 91(3):620–627.

Robertson G. L. 2006. Food Packaging Principles and Practice. Taylor and Francis Group.

Tsimpanogiannis I.N., Y. C. Yortsos. 2002. Model for the gas evolution in a porous medium driven by solute diffusion. *AIChE Journal* 48(11): 2690–2710.

Hybrid Expert System/Analytic Hierarchy Process for Material Selection in Flexible Packaging Structures—Part 2

DUNCAN DARBY

Department of Packaging Science, Clemson University, Clemson, South Carolina 29634

ABSTRACT: In this work, a computer system was created for material selection in the flexible packaging industry that combines expert system technology and decision theory, specifically the analytic hierarchy process. The decision theory part of the work can be turned off (single structure mode) or on (multiple structure mode) by menu selections. When in multiple structure mode, it exists in concert with the expert system. In this mode, the system looks at several structures and runs the expert system to select materials for each generic structure. Then, it applies user-selected criteria (determined in advance) to choose among the structures. Criteria used were cost, competition (multiple suppliers), availability of capacity, environmental friendliness, water vapor barrier and oxygen barrier. In testing, this system was capable of distinguishing changes in the perspective of the user and applying it to the problem at hand to make selections. Sensitivity studies were conducted to demonstrate the system's ability to be appropriately responsive to perspective changes such a supplier vs. purchaser. The module was also tested on several examples that show its capability to make decisions. It was able to select a single best option in most cases.

INTRODUCTION

SELECTION of a flexible packaging structure for a given packaging application is often an exercise in considering among multiple options. Given two flexible packaging structures for a given application, the first inclination may be to say that the cheapest structure will be selected. However, this is often only true in cases where the two materials function in an identical manner. If barriers of one structure are worse than another, and shelf-life is reduced, the savings generated by the lower cost can quickly be consumed by higher costs of expired product.

Likewise, environmental considerations, competition between suppliers and availability of materials can influence the decision between

1557-7244/07/04 213-14

flexible packaging options. The current trend to move away from PVC as a packaging material is not an economic decision, but one that reflects a public perception (perhaps correct or perhaps not) that PVC is environmentally less desirable than other materials. Some consumer goods companies prefer to have multiple suppliers who can make a given structure in order to be able to utilize competition between suppliers. Additionally, a packaging structure that includes materials that are in limited supply will be less desirable to packagers than one whose materials are readily available.

These decisions are often made on a case-by-case basis, and a consistent decision-making system does not necessarily exist. Research was conducted into the possibility of utilizing a computerized decision theory system in this process. The research was conducted at Alcan Packaging in Shelbyville, Kentucky in conjunction with a doctoral dissertation at the University of Louisville. This research was conducted as a part of a larger research program of utilizing an expert system for material selection in flexible packaging.

DECISION THEORY AND THE ANALYTIC HIERARCHY PROCESS

Most decision theory problems involve ranking a set of options against a set of criteria. The criteria themselves are seldom equally ranked, so a system must exist to determine the weight of each criterion. Also, a system must exist to determine how well each option satisfies each criterion. [1]

Thus, the overall value of an option,designated as $v(a)$, is often determined by the adding up the products of criteria weights, k_i, and values, $u_i(a)$.

$$v(a) = k_1 u_1(a) + k_2 u_2(a) + \dots + k_n u_n(a) \tag{1}$$

where, $v(a)$ = overall score of option a, k_i = weight of criterion i, and $u_i(a)$ = value of option a with respect to criterion i.

There are many methods for determining the values of the criteria weights, k_i, for each criterion and the values, u_i, for each option's score against a criterion. There is much debate over the advantages and disadvantages of the various systems and some believe that no decision-mak-

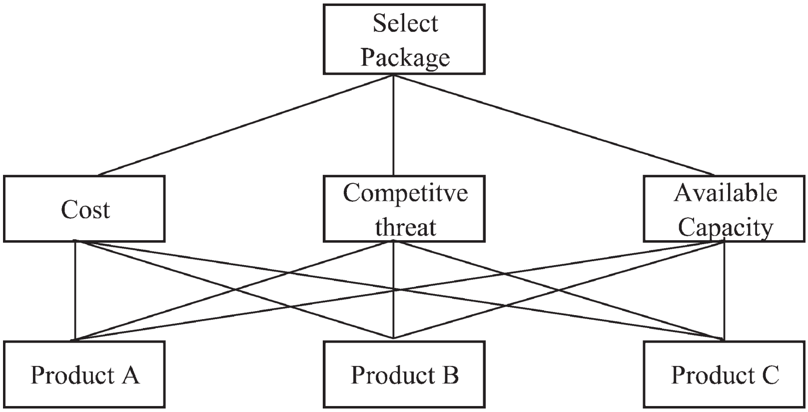

Figure 1. *Example of a Hierarchy Diagram.*

ing system is completely ideal [2]. One of these methods, which has been the subject of considerable research in the past 30 years, is the analytic hierarchy process (AHP). Introduced by Saaty in 1972, the AHP requires that each criterion be compared to all other criteria on a one-to-one basis. It also requires that each option be compared to each other option for its value with respect to each criterion [3]. This is depicted for a flexible packaging problem in Figure 1.

The convention used in AHP for comparing the criteria and options is shown in Table 1. The AHP system requires that, if an option is considered strongly more important than another (an intensity of 5), then the other option must be ranked as 1/5 with respect to the first option. Also, the diagonal of the matrix, where each option is compared to itself, is filled with 1 [3]. This results in a matrix as shown in Table 2.

Table 1. *AHP Numerical Rating Scheme (Saaty and Vargas, 1994).*

Intensity of Importance	Definition
1	Equal importance
2	Weak
3	Moderate importance of one over the other
4	Moderate plus
5	Strong importance
6	Strong plus
7	Very strong importance
8	Very very strong
9	Extreme importance

Table 2. Example Matrix of Criteria Rankings.

	Cost	Capacity	Competitive Threat	Eigenvector (weights, k_i)
Cost	1	5	4	**0.687**
Capacity	1/5	1	2	**0.186**
Competitive Threat	1/4	1/2	1	**0.127**

Inconsistencies in estimation are allowed in the AHP [3]. For example, in Table 2, cost is ranked as more important than capacity by a factor of 5 and more important than competition by a factor of 4. To be consistent, the pairwise comparison of capacity and competition should be 5/4. However, it is 2 on the table. The system allows for this inconsistency and the actual weight assigned with such a discrepancy will end up somewhere between these two values.

The eigenvector of the matrix in Table 2 is calculated using matrix mathematics. An example of this calculation can be found in Golden, Wasil and Harker [2]. This eigenvector is utilized as the weights, (k_i's) from Equation 1. The mathematical significance of this eigenvector is the subject of controversy in the literature [1,2,3], but from a practical standpoint, it amounts to a sophisticated "averaging" of the preferences in Table 2. The calculation is sensitive enough to be influenced by the inconsistencies outlined in the previous paragraph.

A matrix for each criterion, where the options are all compared in a similar pairwise manner, is shown in Table 3. Again, eigenvectors are calculated. These are used as the values, u_i, from Equation 1 [3].

Finally, equation 1 can be calculated using k_i's from Table 2 and u_i's from Table 3. The best option is that which has the highest value, v. This is shown in Table 4.

DESIGN OF THE COMPUTERIZED DECISION MAKING SYSTEM

The computerized decision system allowed for the user to select from the five criteria shown in Table 5. This was a separate computer module, (comparable to setting preferences in commercial software) designed to be run before an actual decision session. After selecting the criteria, the user was required by the program to compare the criteria (as demonstrated in Table 2) in order to establish the weights, k_i, of Equation 1.

Table 3. *Pairwise Comparisons of Options and Resultant Values.*

Cost Matrix	Product A	Product B	Product C	Eigenvector (values, u_i)
Product A	1	3	5	**0.637**
Product B	1/3	1	3	**0.258**
Product C	1/5	1/3	1	**0.105**
			C.R.	**0.033199216**

Cost Matrix	Product A	Product B	Product C	Eigenvector (weights, u_i)
Product A	1	1/3	3	**0.25**
Product B	3	1	5	**0.637**
Product C	1/3	1/5	1	**0.105**
			C.R.	**0.081**

Cost Matrix	Product A	Product B	Product C	Eigenvector (weights, u_i)
Product A	1	1/5	4	**0.194**
Product B	5	1	9	**0.743**
Product C	1/4	1/9	1	**0.063**
			C.R.	**0.061**

The system was developed along with a material selection expert system that selected the specific materials to be used for a given generic structure. When utilizing the AHP part of the system, multiple generic structures were selected. Examples of generic structure are "Film/Ext/Film" for a two layer extrusion laminated film structure or "Film/Adh/Foil/Adh/Film" for a three layer adhesive laminated structure with two films and a foil. The expert system then selected the appropriate materials for each generic structure selected. From this information, the structure material cost and barriers could be calculated. All of

Table 4. *Results of the AHP Example.*

	Cost	Capacity	Competitive Threat	Score Results	Rank
Weights	0.687	0.186	0.127		
Product A	0.637	0.258	0.194	0.510	1
Product B	0.258	0.637	0.743	0.390	2
Product C	0.105	0.105	0.063	0.099	3

Table 5. Criteria for Flexible Packaging Structure Decision.

Criteria	Comment
Cost	Calculated-Materials only MSI cost
WVTR	Calculated based on layers
O_2TR	Calculated based on layers
Environmental Friendliness	Used formulas for environmental reputation, factored in co-mingling
Capacity	Compare products based on available capacity
Competition	Is this a unique product or can others make it?

this information was stored in databases that would later be accessed by the decision system.

As stated, the barrier and material cost information were calculated based on the individual layers selected by the expert system. System rules were then applied to fill out the matrix. As an example, one of the rules stated that a cost difference of 10 or 25 % might make one structure strongly more valued (a value of 5 in Table 1) than another.

Capacity, competition and environmental factors, which are dependent on both the generic structure and the individual materials, were calculated for each structure in the decision-making system. Again, scores were established for the structures and then rules were employed to set the AHP matrix values to fit in with Table 1.

Once the values were determined, Equation 1 was calculated for each structure and the best structure was recommended.

METHOD OF EVALUATING THE SYSTEM

Important measurements of a decision making system include the ability to change the decision when the weights or values of equation 1 change (sensitivity) and the ability to reach a decision [1]. These abilities were tested with this system.

The analytic hierarchy process provides a structured method for a decision maker to think about the criteria that are important to a decision and to compare their relative importance [3]. The relative importance, (k_i in Equation 1) which is assigned to a criterion can be highly dependent on point of view. For instance, a supplier of packaging material might like to specify a package that only he can make (little competition), can be readily manufactured (open capacity), and is priced at a level where profit can be generated. In spite of the need for profit, the supplier might choose to make less money on something where they are the only manufacturer in order to prevent competition.

The purchaser, on the other hand, might prefer a product that is made by several people (healthy competition), can be readily bought (open capacity) and is available at the lowest possible price. In order to hedge against the risks entailed when there is only one supplier, the purchaser might sometimes prefer to pay a somewhat higher price to buy a product manufactured by multiple suppliers.

To be a functional decision system, the AHP module should neither under-react nor over-react to changes in preference. In order to test the sensitivity of the AHP portion of the system to this type of difference in points of view, a product was selected (ketchup) for which there are multiple valid structures. The possible generic structures used and the background for the sensitivity study are shown in Table 6.

Two experiments were designed, utilizing the criteria from Table 5. The criterion weights were varied in order to consider cases from a multiple perspectives as outlined above. In the first experiment, cost, capacity, availability and environmental friendliness were utilized as criteria In the second experiment, cost, environmental friendliness and barrier properties were included because the barriers for the different structures covered enough of a range to change the rankings.

Once the sensitivity was evaluated, the system was then tested to see if it could successfully choose between options. Ten representative cases were explored with respect to the analytic hierarchy process part of the system. These were cases for which there is more than one valid structure currently supplied in the industry. These cases are shown in Table 8.

Table 6. *AHP Sensitivity Study Parameters.*

Generic packaged product:	Condiment
Specific packaged product:	Ketchup
Fill weight, oz.:	0.5 oz.
Package type:	4 seal flat pouch
Opened width, in.:	3
Repeat length, in.:	3
Machine type:	VFFS jaw drive
Print resolution:	low resolution
Structures chosen:	Fi/Adh/Fi
	Fi/Adh/Fo/Ext
	Fi/Adh/Fo/Ext/Fi
	Fi/Ext/Fi
Repeat length, in.:	0.03125

Table 7. AHP Sensitivity Study Preference Matrices.

Experiment 1

Preference Matrix A—Stong Cost Preference Over "Soft" Criteria

	Cost	Capacity	Competition	Environmental
Cost	1	7	7	9
Capacity	1/7	1	1	5
Competition	1/7	1	1	1
Environmental	1/9	1/5	1	1

Preference Matrix B—Cost Equal with Available Criteria

	Cost	Capacity	Competition	Environmental
Cost	1	1	1	5
Capacity	1	1	1	4
Competition	1	1	1	5
Environmental	1/5	1/4	1/5	1

Experiment 2

Preference Matrix C—Stong Cost Preference Over "Soft" Criteria

	Cost	Capacity	Competition	Environmental
Cost	1	7	7	7
Environmental	1/7	1	2	2
WVTR	1/7	1/2	1	1
O_2TR	1/7	1/2	1	1

Preference Matrix D—Product Protection Over Cost

	Cost	Capacity	Competition	Environmental
Cost	1	7	1/3	1/3
Environmental	1/7	1	1/7	1/7
WVTR	3	7	1	1
O_2TR	3	7	1	1

Table 8. *Test Base for Functionality of AHP Module.*

Problem	Group	Generic Product	Package Type	Comment
A1	condiment	ketchup	4 seal flat pouch	Liquid-solid blend in pouch
A2	condiment	barbeque sauce	Roll fed lidding	Liquid-solid blend in cup
A3	confection	chocolate bar	Sealable tube wrapper	Confection needing little barrier
A4	confection	granola bar	Sealable tube wrapper	Confection needing barrier
A5	dairy	yogurt	Roll fed lidding	Comparison to test environmental aspects
A6	dry beverage	coffee ground	3 seal flat pouch	Granular solid in pouch
A7	dry beverage	fruit drink mix	3 seal flat pouch	Powdery solid in pouch
A8	liquid beverage	fruit drink	Stand up pouch	Liquidin pouch
A9	snack	potato chips	3 seal tube fin	Snack requiring light barrier
A10	snack	corn chips	3 seal tube lap	Snack requiring little light barrier

This test base was constructed to assure that multiple structures were viable, and also to cover a broad range of applications.

RESULTS OF SYSTEM EVALUATION

The first experimental testing of the AHP decision system was to investigate the sensitivity of the system. Table 9 shows the results of the first sensitivity test. In Preference Matrix A, in which cost was selected as stronger in importance than the "softer" criteria of capacity, competition and environmental, the weight (k_i) applied to the cost was overwhelmingly the largest. However, when the other criteria were treated as equal in importance with cost, the cost weight was nearly equal to the weighting of capacity and competition.

An intentional inconsistency was introduced in Table 8, where capacity and availability, which compared equally with cost, compared slightly differently with environmental friendliness. As a result, the weighting for capacity came out with a slightly lower weighting than cost and competition.

It is interesting to note that, in spite of the fact that the weight of the cost swings from around 70% in Preference Matrix A to around 30% in Preference Matrix B, the rankings of the four structures did not change. This is because, as can be seen in Table 9, the only numerically large difference between these structures was the cost. In this case, the system would be over-reacting if it were to change the order of preferences.

In the second sensitivity test, the cost was pitted against protection of the packaged product quality (barriers) and environmental friendliness. As can be seen in the table, the change in perspective completely changed the rankings in this test. In this case, the barriers have sufficient difference that the weights (k_I's) and values (u_i's) together force the system to choose entirely different results.

The results of these two experiments suggest that the AHP portion of the system is capable of changing its selection when the properties of the structures selected, along with the preferences, dictate that a change should happen. They also indicate that the system should not over-react when these factors do not warrant a change in selection. These results are similar to those found in the literature when sensitivity studies of AHP systems have been conducted [4,5].

The system was next tested on a series of cases, as shown in Table 10, to see if it could pick a single best structure. A preference matrix using

Table 9. *Sensitivity Study Experiment 1.*

	Cost	Capacity	Competition	Environmental	WVTR	O_2TR		
Units	**$/1000 sq.in**	**1–9 Scale**	**1–9 Scale**	**1–9 Scale**	**g/100 sq. in/24 hr**	**cc/100 sq. in/24 hr**		
Weight in 1st Run—Matrix A	0.69153	0.13409	0.13409	0.04028	0	0		
Weight in 1st Run—Matrix B	0.31656	0.29982	0.31656	0.06795	0	0		
			Structure Properties				**Rank for Preference Matrix A**	**Rank for Preference Matrix B**
Structure 1	0.0976	5	5	5	0.323	41.000	2	2
Structure 2	0.1574	3	5	5	0.000	0.000	4	4
Structure 3	0.1421	3	5	5	0.000	0.000	3	3
Structure 4	0.0818	5	5	7	0.768	8.600	1	1

Table 10. *Sensitivity Study Experiment 2.*

	Cost	Capacity	Competition	Environmental	WVTR	O_2TR		
Units	**$/1000 sq.in**	**1–9 Scale**	**1–9 Scale**	**1–9 Scale**	**g/100 sq. in/24 hr**	**cc/100 sq. in/24 hr**		
Weight in 1st Run—Matrix A	0.69578	0	0	0.13987	0.08217	0.08217		
Weight in 1st Run—Matrix B	0.17838	0	0	0.38915	0.38915	0.38915		
			Structure Properties				**Rank for Preference Matrix A**	**Rank for Preference Matrix B**
Structure 1	0.0976	5	5	5	0.323	41.000	2	4
Structure 2	0.1574	3	5	5	0.000	0.000	4	2
Structure 3	0.1421	3	5	5	0.000	0.000	3	1
Structure 4	0.0818	5	5	7	0.768	8.600	1	3

Table 11. *Test of AHP Module Function*

Problem	Group	Generic Product	Package Type	Number of Options	Number of Ranks	How Many Ranked as Nu1mber 1
A1	condiment	ketchup	4 seal flat pouch	6	4	1
A2	condiment	barbeque sauce	Roll fed lidding	3	2	2
A3	confection	chocolate bar	Sealable tube wrapper	2	2	1
A4	confection	granola bar	Sealable tube wrapper	4	4	1
A5	dairy	yogurt	Roll fed lidding	2	2	1
A6	drybeverage	coffee ground	3 seal flat pouch	3	3	1
A7	dry beverage	fruit drink mix	3 seal flat pouch	2	2	1
A8	liquid beverage	fruit drink	Stand up pouch	2	2	1
A9	snack	potato chips	3 seal tube fin	2	2	1
A10	snack	corn chips	3 seal tube lap	2	2	1

all six criteria was prepared and the expert system, along with the AHP module was run. The results are shown in Table 11. The number of options shows how many generic structures were selected and the number of ranks show how many different levels the system assigned. The final column shows whether or not multiple structures were ranked equally as the best option.

As can be seen, the system was able to select a single optimum structure based on the selected criteria in all cases, except for problem A2. Further investigation showed that the two structures that were ranked equally were identical structures except that one was extrusion laminated and the other was adhesive laminated. As it happens, the two structures in question are similar in all properties and the structures' calculated costs were within five percent of one another. The system had been set to view small cost differences as equal in value. Thus, the system ranked them as identical.

CONCLUSIONS

The analytic hierarchy process appears to have some promise as a possible decision-aid in selecting from various flexible packaging options in cases where more factors than cost are considered. Testing of the system suggests that it should be sensitive enough to change depending on a perspective change and yet not over-react. Testing of the system's ability to make a selection also suggests that this system could function as a decision-aid system to narrow the possible field to one option usually and occasionally to two or more equally rated options.

REFERENCES

1. French, S. 1986. *Decision Theory: An Introduction to the Mathematics of Rationality.* Chichester, UK: Ellis Horwood Limited.
2. Bouyssou, D., Marchant, T., Pirlot, M. Perny, P., Tsoukias, A. and P. Vincke. 2000. *Evaluation and Decision Models: A Critical Perspective.* Boston: Kluwer Academic Publishers.
3. Golden, B., Wasil, E. and P. Harker. 1989. *The Analytic Hierarchy Process- Applications and Studies.* Berlin: Springer-Verlag.
4. Saaty, T. 2001. *Decision Making for Leaders.* Pittsburg: RWS Publications.
5. Saaty, T. and L. Vargas. 1994. *Decision Making in Economic, Political, Social and Technological Environments: The Analytic Hierarchy Process.* Pittsburg: RWS Publications.

The Effect of Ventilation and Hand Holes on Loss of Compression Strength in Corrugated Boxes

J. SINGH[1,*], E. OLSEN[3], S. P. SINGH[4], J. MANLEY[2] and F. WALLACE[2]

[1]*Associate Professor, Industrial Technology, Cal Poly State University, San Luis Obispo, CA*

[2]*Research Assistant, Industrial Technology, Cal Poly State University, San Luis Obispo, CA.*

[3]*Assistant Professor, Industrial Technology, Cal Poly State University, San Luis Obispo, CA.*

[4]*Professor, School of Packaging, Michigan State University, East Lansing, MI*

ABSTRACT: Corrugated packaging is used to package approximately 90% of all products that reach retail store shelves and aisles in the United States. A large number of these corrugated shippers are used to ship fresh produce and perishables through the cold-chain environment that requires these boxes to have venting to permit air circulation. In addition, corrugated boxes for that are large in size and contain heavier products, may have hand holes to facilitate manual handling. The presence of ventilation and hand holes both cause a loss of material in two or more faces of the box. As a result the compression strength required for shipping and stacking is compromised and can result in damage to contents. Hand holes that do not meet the appropriate strength requirements can be a safety issue in manual handling if the contents are released when handling. This study was initiated to understand the loss of compression strength in corrugated containers as a function of size, shape and location of ventilation and hand holes used for handling ergonomics and extending shelf life for perishables with good air flow. Based on experimental data, results show that the loss in strength can range between 10 to 40% and is significantly larger than previously reported.

1.0 INTRODUCTION

DUE to its high strength to low weight ratio corrugated packaging is poised as the leading choice for transport packaging in the United States. By some estimates corrugated packaging is used to package approximately 90% of all products for retail distribution in the United

*Author to whom correspondence should be addressed. Email:jasingh@calpoly.edu

1557-7244/07/04 227-12

States [1]. The popularity of corrugated packaging also stems from the fact that it is practical, useful, economical, renewable and recyclable [1]. It is also a substrate that can be custom designed and provides excellent merchandising appeal through printing on box panels. Twede [2] accounted that 80% of the $46 billion worth of paper based packaging used is corrugated fiberboard shipping containers.

Corrugated shippers are designed to overcome the distribution environment hazards so that the products they carry reach the consumers, intact and ready for use. The transportation and warehousing hazards faced commonly by corrugated shippers include compression, shock, vibration, temperature, creep and humidity among others. Corrugated shippers often have holes to allow for ventilation to perishables and permit air circulation in the cold chain shipping and storage environments. In addition packaging designers may offer hand holes to permit manual handling of boxes that are either large in size or carry heavy products. The hand holes often improve ergonomics and assist in handling associated with large or awkwardly designed containers. It is important that the strength of the hand hole be sufficient so that the contents are not released during exposure to normal stresses that are likely to occur during manual handling. Failure of a hand hole structure on a corrugated box can release the contents causing damage or injury.

Some guidelines for designing hand holes for corrugated boxes are provided by ASTM D 6804, which is a standard guide for "Hand Hole Design in Corrugated Boxes" and is intended to test the performance of hand hole strength [3]. It provides guidelines for designing pre-cut apertures intended for use as hand holes in corrugated boxes during manual handling of boxed cargo. Although this standard offers guidance for package development and for subsequent testing of boxes to measure performance, it is not intended to provide specific information on the design of hand holes [3]. The standard recommends that the designers follow best practices when designing hand holes for corrugated shippers but also take into consideration the product and package weight when deciding on the proper use of a hand hole.

It is obvious that removing any material from the load bearing vertical faces of a container would lead to a decrease in its overall compression strength. This paper concentrates on evaluating the effect of eliminating controlled amounts of corrugated material, in the forms of ventilation and hand holes, from RSC style boxes on the overall compression strength of the container. The purpose of this study was to establish a relationship that can be used to correlate the percentage of corrugated material removed from the sidewalls of containers to the loss of compression strength of the container. While it has been obvious and known that both ventilation and hand holes produce a loss of box strength, there has been very little published information quantifying this loss.

In a recent study by Han and Park [4], finite element analysis (FEA) was used to predict the loss of compression strength due to vent and hand holes. The authors also used actual testing on fifteen different styles of boxes and hole patterns. The study used double-walled corrugated boxes with dimensions of $41 \times 30 \times 25$ cm and the surface area occupied by the holes was approximately 2% of the total surface area of the vertical faces of the boxes. The study reported a compression strength loss of less than 10% based on FEA and experimental data. However, there are a few limitations of this study. It has been the experience of the authors of the present research that compression strength losses for single-walled corrugated boxes exceed 10% due to the presence of any type of ventilation or hand holes. The difference between the results reported between the past publication [4] and the present study is very likely due to the structural differences such as the number of walls and the dimensions of the boxes tested as well as the surface area covered by the holes on the vertical walls. The present study focuses on single-walled corrugated containers that are used in more than 90% of all applications in the US. [1]

This study evaluated the following two objectives:

1. Effect of location of ventilation or hand holes in corrugated shippers on loss of compression strength
2. Effect of shape and size of ventilation or hand holes in corrugated shippers on their loss of compression strength

2.0 MATERIALS AND METHOD

2.1 Corrugated Boxes

All corrugated box samples used for this study were created using ArtiosCAD software and the Premium Line 1930 model of the Kongsberg table (Esko Graphics, Ludlow, Massachusetts, USA). Single-walled Regular Slotted Container style (FEFCO 0201) boxes measuring 50.8 cm $\times$ 40.64 cm $\times$ 25.4 cm were used for this study. The corrugated fiberboard used was C-flute with basis weight of 215/162/215 g/m2, bursting strength of 12.70 kgf/cm², and edge crush test (ECT) value of 8.09 kgf/cm. All boxes had the flutes running in the top to bottom direction in the assembled stage. All samples were conditioned at 23 ± 1 °C and 50% relative humidity for 48 hours prior to testing in accordance with ASTM D4332 [5]. Five replicates for all variations of hand holes and vent holes were tested for compression strength.

All compression tests were conducted using a Lansmont Model 152-30 compression test system (Lansmont Corporation, Monterey, CA, USA) and in accordance with ASTM D642 [6]. A preload of 22.68 kgf was applied to all specimens prior to observing the compression strength values. The fixed-platen mode of the compression tester was used to conduct all testing at a speed of 12.7 ± 2.5 mm/min until failure was observed.

2.2 Hand Holes

For this phase of testing, a standard sized (8.89 cm × 2.54 cm) hand hole was cut out on the smaller opposite vertical faces of the RSC containers. The goal of this phase was to attempt to identify any relationship between the location of the hand hole and the overall compression strength of the container. The locations of the hand holes are shown in

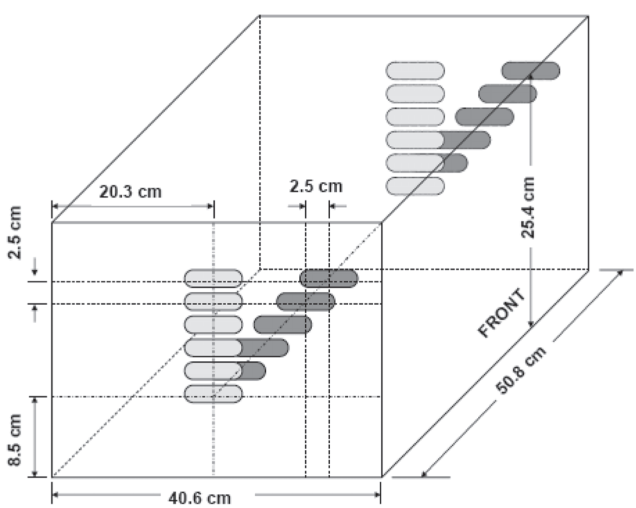

Figure 1. *Hand Hole Locations.*

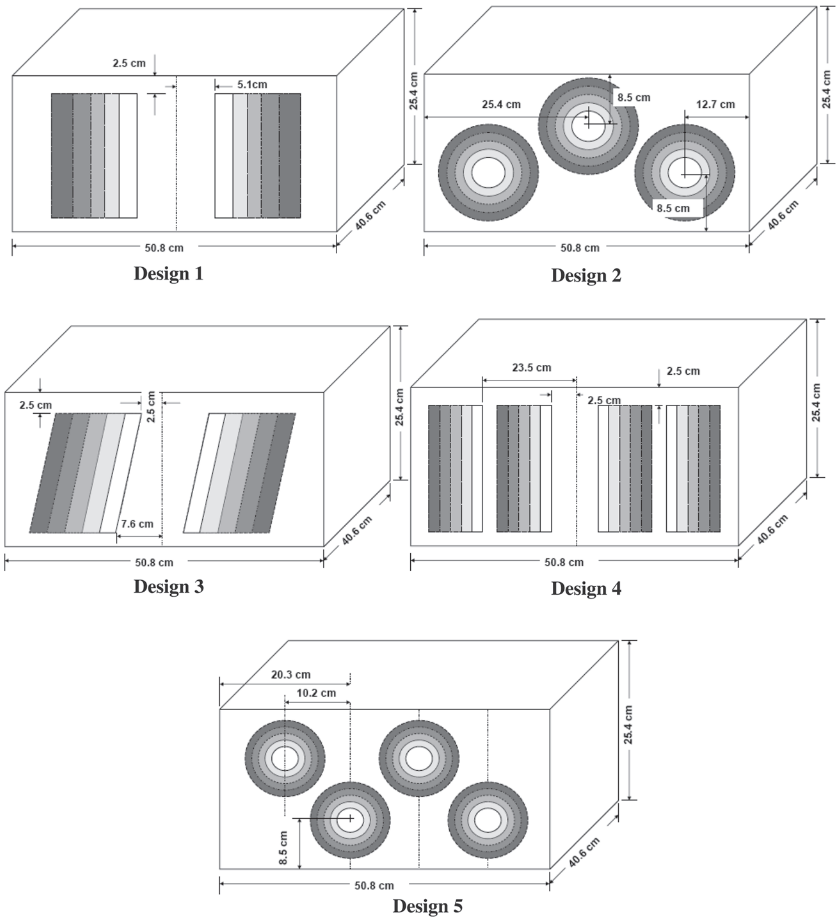

Figure 2. *Vent Hole Design Specifications.*

Figure 1. For the vertical locations, the lowest position started at 8.47 cm from the center of the bottom (one third of the height of the container from the bottom). The remaining hand holes were cut out at a distance of 2.54 cm from this starting position. For the diagonal locations, the starting (bottom) location was the same as that for the vertical hand holes. The remaining five locations were placed along the diagonal line that went through an upper corner of the face through the center of the bottom-most hand hole, at a vertical distance of 2.54 cm between every subsequent location.

All locations of the hand holes were symmetric for both short faces on which they were cut out. Compression tests were conducted for five replicates of each configuration of the hand holes. A total of twelve designs were tested.

2.3 Vent Holes

This part of the study examined the relationship between the increasing vent hole sizes placed on the largest vertical faces of the corrugated containers to the decreasing compression strength of the container. To achieve this, five vent designs were created and each design had five variations, which removed 10%, 20%, 30%, 40% and 50% of the corrugated material from the side panels. Figures 2 and 3 show the details of the size and shape of vent holes tested.

Table 1 shows the dimensions for all vent hole designs as related to the percentage of material removed from that face. The compression tests were conducted for five replicates of each configuration of the hand holes.

Figure 3. *Vent Hole Test Samples.*

Table 1. *Vent Hole Dimensions.*

Area Removed*		Vent Hole Dimensions - cm and (Quantity per Side)				
%	cm^2	Design 1(2×)	Design 2(3×)	Design 3(2×)	Design 4(4×)	Design 5(4×)
10	129	3.2*20.3	R = 3.70	3.2*20.3	1.6*20.3	R = 3.2
20	258	6.4*20.3	R = 5.23	6.4*20.3	3.2*20.3	R = 4.5
30	387	9.5*20.3	R = 6.41	9.5*20.3	4.8*20.3	R = 5.6
40	516	12.7*20.3	R = 7.40	12.7*20.3	6.4*20.3	R = 6.4
50	645	15.9*20.3	R = 8.27	15.9*20.3	7.9*20.3	R = 7.2

*Area removed reflects the total surface area cut out of the vertical faces for the vent holes.

3.0 RESULTS & DISCUSSION

3.1 Hand Holes

Table 2 shows the means and standard deviations for the compression testing results for the twelve different hand hole locations as compared to the relative values for control samples. The mean and standard deviations for controls (no material removed from vertical faces) were: peak compression force of 2587 and 60 N and peak deflection of 0.49 and 0.02 cm respectively. Five samples were tested for each variable studied.

Regression analyses of the vertical and diagonal distance data and their interaction did not indicate a significant relationship between hand hole location and compressive force or deflection. Table 2 shows the

Table 2. *Compression Test Results for Vent Holes.*

Vertical Distance (cm)	Diagonal Distance (cm)	0.0		2.0		3.9		5.9		7.8		9.8		11.7	
		Force and Deflection % Control Values													
		Force (N)	Deflect (cm)	Force (N)	Deflect (cm)	Force (N)	Deflect (cm)	Force (N)	Deflect (cm)	Force (N)	Deflect (cm)	Force (N)	Deflect (cm)	Force (N)	Deflect (cm)
0.0	mean	99	115												
	std dev	170	257												
	n	4													
1.6				98	98										
				183	101										
				5											
2.5		95	120												
		136	132												
		5													
3.3						101	101								
						114	65								
						5									
4.9								101	101						
								135	108						
								5							
5.1		98	117												
		198	209												
		4													
6.5										102	104				
										121	84				
										5					
7.6		99	119												
		195	208												
		3													
8.1												101	103		
												129	113		
												4			
9.8														102	100
														129	151
														4	
10.2		97	96												
		158	207												
		4													
12.7		97	101												
		115	209												
		4													
All		**98**	**111**	**98**	**98**	**101**	**101**	**101**	**101**	**102**	**104**	**101**	**103**	**102**	**100**
		162	**204**	**183**	**101**	**114**	**65**	**135**	**108**	**121**	**84**	**129**	**113**	**129**	**151**
		24		**5**		**5**		**5**		**5**		**4**		**4**	

Notes: (1) Outliers removed from table
(2) Mean and standard deviation for controls (zero material removed):Compression = 2587, 60 N Deflection =0 .49, 0 .02 cm

weak relationship between the compressive force and each vertical and diagonal location.

3.2 Ventilation Holes

Table 3 shows the means and standard deviations for the compression testing results for the five designs for vent holes tested as compared to the relative values for control samples. Each design had five different percentages of material removed and five samples were tested for each configuration.

The data were analyzed first using a 2-way analysis of variance. As expected, the designs, percent material removed, and their interaction were significant ($p = 0.000$). The strength of each design reduced in a linear fashion in correlation with the percent of material removed. Individual regression analyses for each design were significant ($p = 0.000$) and had

Table 3. *Compression Test Results for Vent Holes.*

			Design					
			1	2	3	4	5	All
			Compression Strength % Control Value (N)					
Material Removed (%)	10	mean	79	79	85	82	77	80
		std dev	74	79	101	40	76	74
		n	5	5	5	5	5	25
	20		77	62	75	73	64	70
			145	86	56	35	67	78
			5	5	5	5	5	25
	30		73	53	67	63	54	62
			119	72	126	51	85	90
			5	5	5	5	5	25
	40		65	44	60	53	45	53
			78	50	86	77	87	75
			5	5	5	5	5	25
	50		55	34	47	*	33	42
			127	42	59	*	65	73
			5	5	5	0	5	20
	All		70	54	67	68	55	62
			109	66	86	51	76	78
			25	25	25	20	25	120

Notes:
(1) Outliers removed from table
(2) Mean and standard deviation for controls (zero material removed) = 4177, 141N.

adjusted r-squared values ranging from 78.4% to 97.3% indicating a good fit to a linear model (Table 4).

One way to compare the compression strength performance of the various designs is to examine the regression coefficients for the percent material removed versus the parentage reduction in compression strength from the control units. The control units had no venting. The five control units had an average strength of 4177 N. Table 4 shows coefficients for the intercept and the percent material removed variable. A significant positive intercept value can be interpreted as a "zero percent removed" design penalty. For example, Design 1 predicts a 12% reduction in strength even if the percent of material removed is zero. It should be pointed out that predicted strength values based on the coefficients in Table 4 are only applicable within the material removal range tested (10–50%). Design 4 became unstable at the 50% level. These five data points, showing approximately an 80% strength reduction as shown in Figure 4, were removed to calculate the values in Table 4.

A reasonable expected value for the percent material removed coefficient would be 1.0. This means that predicted compression strength reduced the same percentage as the material removed. A coefficient higher than 1.0 means that strength is being reduced faster than material is being reduced. A coefficient less than 1.0 means that strength is being reduced proportionally less. For example in Design 1, strength is reduced by 0.56% for every 1.0% of material removed on average. Alternatively, both circular designs reduce in strength by 1.08% for every 1% of material removed.

All of the mean strength reduction values shown in Table 4 are signifi-

Table 4. *Regression Results for Vent Holes Sorted by Mean Strength Reduction.*

	Coefficients			
	Intercept	**% Material Removed**	**Adjusted R-Sq**	**Mean Strength Reduction % (1)**
Design 1	0.12	0.59	78%	30.1%
Design 4 (2)	0.08	0.96	98%	32.3%
Design 3	0.06	0.91	95%	33.2%
Design 5	0.13	1.08	97%	45.5%
Design 2	0.13	1.08	96%	45.5%

Notes:
(1) Expected value for strngth reduction equal to materil reduction is 30%.
(2) Desikgn not linear above 40% material removal.

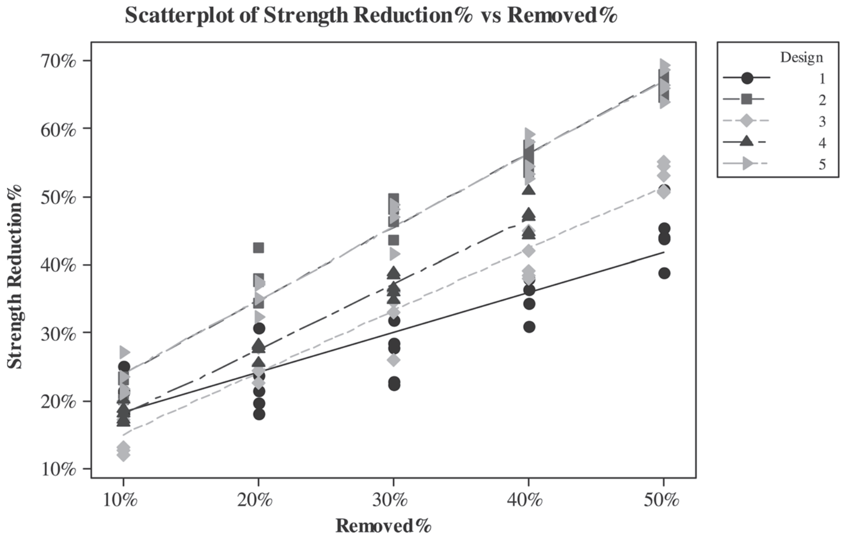

Figure 4. *Regression Plots for Vent Hole Tests.*

cantly different, except for the two circular shapes: Designs 2 and 5. The order of the designs in Table 4 has interesting implications for vent hole design. Rectangular holes seem to offer significant strength advantages over circular holes. Even the parallelogram Design 3 is significantly better than the circular designs. This is interesting in that one might expect that designs with corners would be at a disadvantage because of corner tendency to add to stress concentrations. This is a possible explanation why Design 4 with 4 rectangular cutouts per side performed more poorly that Design 2 with only 2 cutouts.

4.0 CONCLUSIONS

1. The presence of ventilation and hand holes can cause strength reduction between 20 to 50% in single wall corrugated shipping containers.
2. The shape of the hole is critical in loss of strength. Vertical holes that are rectangular or parallelogram in shape are better in retaining corrugated box strength as compare to circular holes.
3. A linear relationship exists between the loss of strength and the total area of the holes made for venting or handling. This relationship does not stay linear when over 40% of the face material is removed.

5.0 REFERENCES

1. International Corrugated Packaging Foundation, Corrugated Curricula—Course Materials on Corrugated Packaging, http://www.icpfbox.org/, accessed February 4, 2008.
2. Twede, D. and S. Selke, *Cartons, Crates and Corrugated Board: Handbook of Paper and Wood Packaging Technology,* ISBN No: 1-932078-42-8, DEStech Publications Inc., Lancaster, PA USA, 2005.
3. ASTM D6804, Standard Guide for Hand Hole Design in Corrugated Boxes, Vol. 15.10, American Society of Testing and Materials, West Conshohocken, PA, USA, 2007.
4. Han, J. and J. M. Park, Finite Element Analysis of Vent/Hand Hole Designs for Corrugated Fiberboard Boxes, *Packaging Technology and Science,* 2007, Volume 20, Issue 1: 39–47.
5. ASTM D4332, Standard Practice for Conditioning Containers, Packages, or Packaging Components for Testing, Vol. 15.10, American Society of Testing and Materials, West Conshohocken, PA, USA, 2007.
6. ASTM D642, Standard Test Method for Determining Compressive Resistance of Shipping Containers, Components, and Unit Loads, Vol. 15.10, American Society of Testing and Materials, West Conshohocken, PA, USA, 2007.

GUIDE TO AUTHORS

1. Manuscripts shall be sent electronically to the editor, Prof. Stanley Dunn at smd@occlusal.rutgers.edu using Microsoft Word in an IBM/PC format. If electronic submission is not possible, three paper copies of double-spaced manuscripts may be sent to Stan Dunn, Editor of the *Journal of Applied Packaging Research*, 98 Brett Road, Piscataway, NJ 08854, USA (Telephone 732-445-4462). Manuscripts should normally be limited to the space equivalent of 6,000 words. The editor may waive this requirement in special occasions. As a guideline, each page of a double-spaced manuscript contains about 300 words. Include on the title page the names, affiliations, and addresses of all the authors, and identify one author as the corresponding author. Because communication between the editor and the authors will be electronic, the email address of the corresponding author is required. Papers under review, accepted for publication, or published elsewhere in journals are normally not accepted for publication in the *Journal of Applied Packaging Research.* Papers published as proceedings of conferences are welcomed.
2. Article titles should be brief, followed by the author's name(s), affiliation, address, country, and postal code (zip) of author(s). Indicate to whom correspondence and proofs should be sent, including telephone and fax numbers and e-mail address.
3. Include a 100-word abstract and keywords.
4. If electronic art files are not supplied, submit three copies of camera-ready drawings and glossy photographs. Drawings should be uniformly sized, if possible, planned for 50% reduction. Art that is sent electronically should be saved in either a .tif or .JPEG files for superior reproduction. All illustrations of any kind must be numbered and mentioned in the text. Captions for illustrations should all be typed on a separate sheet(s) and should be understandable without reference to the text.
5. DEStech uses a numbered reference system consisting of two elements: a numbered list of all references and (in the text itself) numbers in brackets that correspond to the list. At the end of your article, please supply a numbered list of all references (books, journals, web sites etc.). References on the list should be in the form given below. In the text write the number in brackets corresponding to the reference on the list. Place the number in brackets inside the final period of the sentence cited by the reference. Here is an example [2].

   Journal: 1. Halpin, J. C., "article title", *J. Cellular Plastics,* Vol. 3, No. 2, 1997, pp. 432–435.
   Book: 2. Kececioglu, D. B. and F.-B. Sun. 2002. *Burn-In Testing: Its Quantification and Optimization,* Lancaster, PA: DEStech Publications, Inc.

6. Tables. Number consecutively and insert closest to where first mentioned in text or type on a numbered, separate page. Please use Arabic numerals and supply a heading. Column headings should be explanatory and carry units. (See example at right.)

Table 5. Comparison of state-of-the-art matrix resins with VPSP/BMI copolymers.

Resin System	Core Temp. (DSC peak)	Char Yield, %
Epoxy (MY720)	235	30
C379: H795 = 1.4	285	53

7. Units & Abbreviations. SI units should be used. English units or other equivalents should appear in parentheses if necessary.
8. Symbols. A list of symbols used and their meanings should be included.
9. Page proofs. Authors will receive page proofs by E-mail. Proof pages will be in a .PDF file, which can be read by Acrobat Reader. Corrections on proof pages should be limited to the correction of errors. Authors should print out pages that require corrections and mark the corrections on the printed pages. Pages with corrections should be returned by FAX (717-509-6100) or mail to the publisher (DEStech Publications, Inc., 439 North Duke Street, Lancaster, PA 17602, USA). If authors cannot handle proofs in a .PDF file format, please notify the editor, Stan Dunn at smd@occlusal.rutgers.edu.
10. Index terms.With proof pages authors will receive a form for listing key words that will appear in the index. Please fill out this form with index terms and return it.
11. Copyright Information. All original journal articles are copyrighted in the name of DEStech Publications, Inc. All original articles accepted for publication must be accompanied by a signed copyright transfer agreement available from the journal editor. Previously copyrighted material used in an article can be published with the *written* permission of the copyright holder (see #14 below).
12. Headings. Your article should be structured with unnumbered headings. Normally two headings are used as follows:

    Main Subhead: DESIGN OF A MICROWAVE INSTALLATION
    Secondary Subhead: Principle of the Design Method

    If further subordination is required, please limit to no more than one (*Third Subhead*).

13. Equations. Number equations with Arabic numbers enclosed in parentheses at the right-hand margin. Type superscripts and subscripts clearly above or below the baseline, or mark them with a caret. Be sure that all symbols, letters, and numbers are distinguishable (e.g., "oh" or zero, one or lowercase "el," "vee" or Greek nu).
14. Permissions. The author of a paper is responsible for obtaining releases for the use of copyrighted figures, tables, or excerpts longer than 200 words used in his/her paper. Copyright releases are permissions to reprint previously copyrighted material. Releases must be obtained from the copyright holder, which is usually a publisher. Forms for copyright release will be sent by the editor to authors on request.

General: The *Journal of Applied Packaging Research* and DEStech Publications, Inc. are not responsible for the views expressed by individual contributors in articles published in the journal.